

The global wildland–urban interface

<https://doi.org/10.1038/s41586-023-06320-0>


Received: 12 May 2023

Accepted: 14 June 2023

Published online: 19 July 2023

Open access

 Check for updates

Franz Schug¹, Avi Bar-Massada², Amanda R. Carlson³, Heather Cox¹, Todd J. Hawbaker³, David Helmers¹, Patrick Hostert^{4,5}, Dominik Kaim⁶, Neda K. Kasraee¹, Sebastián Martinuzzi¹, Miranda H. Mockrin⁷, Kira A. Pfoch¹ & Volker C. Radeloff¹

The wildland–urban interface (WUI) is where buildings and wildland vegetation meet or intermingle^{1,2}. It is where human–environmental conflicts and risks can be concentrated, including the loss of houses and lives to wildfire, habitat loss and fragmentation and the spread of zoonotic diseases³. However, a global analysis of the WUI has been lacking. Here, we present a global map of the 2020 WUI at 10 m resolution using a globally consistent and validated approach based on remote sensing-derived datasets of building area⁴ and wildland vegetation⁵. We show that the WUI is a global phenomenon, identify many previously undocumented WUI hotspots and highlight the wide range of population density, land cover types and biomass levels in different parts of the global WUI. The WUI covers only 4.7% of the land surface but is home to nearly half its population (3.5 billion). The WUI is especially widespread in Europe (15% of the land area) and the temperate broadleaf and mixed forests biome (18%). Of all people living near 2003–2020 wildfires (0.4 billion), two thirds have their home in the WUI, most of them in Africa (150 million). Given that wildfire activity is predicted to increase because of climate change in many regions⁶, there is a need to understand housing growth and vegetation patterns as drivers of WUI change.

Humans have greatly affected the Earth's land surface in recent centuries^{7–11}. In particular, the expansion of the built environment and the growth of settlements and their long-term resource requirements have been dramatic across the globe^{12–14}. The growth of settlements can have remote effects via teleconnected processes^{15,16} but the most immediate human–environmental conflicts arise where buildings are built in or near wildland vegetation, an area known as the wildland–urban interface (WUI)^{1,17}. The WUI is widespread across Australia, Europe and North America^{18–22} and there is evidence for WUI in some other countries^{23–26}. However, the worldwide distribution of the WUI is unknown².

The WUI is a desirable place to live for many people as a result of its proximity to natural amenities but it is also an area of manifold hazards to both humans and natural ecosystems. Wildfires are a particular threat to houses and lives, often caused by human ignition and facilitated by altered fire regimes where settlements sprawl into fire-dependent ecosystems. The availability of buildings themselves as fuel, along with swiftly moving fire, makes evacuations difficult^{19,27–29}. Indeed, the number of wildfires has increased in the WUI over the past few decades² owing to both housing growth and climate change. Other hazards to humans or their environment include the loss of biodiversity and carbon storage due to habitat loss and fragmentation, predation of wildlife by cats and dogs, light and noise pollution, the introduction of invasive species, an increased risk for the spread of zoonotic diseases and changes in hydrology^{3,30–33}. Quantifying any of these hazards requires a consistent global assessment of the WUI. This is particularly important because the number of exposed buildings and people in the WUI is expected to grow as population grows and because climate change is

expected to further increase the risk for many of these hazards, such as higher wildfire frequency and intensity^{18,34,35}.

Here, we present a global map of the 2020 WUI at 10 m resolution using a globally consistent and validated approach based on remote sensing-derived datasets of building area⁴ and wildland vegetation⁵. We distinguished between two types of WUI: intermix WUI (where buildings and wildland vegetation intermingle) and interface WUI (where buildings are close to large wildland vegetation patches). We further distinguished between WUI dominated by forest, shrubland and wetland versus that dominated by grassland. We then summarized population and biomass in the WUI for each country and biome, using the biome definition of ref. 36. To identify areas of increased fire hazard in the WUI, we assessed wildfire occurrence using two remote sensing-based datasets—Moderate Resolution Imaging Spectroradiometer (MODIS) Active Fire data for 2003–2020 and Visible Infrared Imaging Radiometer Suite (VIIRS) Active Fire data for 2013–2020. Our identification of WUI types by dominant land cover allowed for a regionalized evaluation of fire hazard in the WUI. For example, whereas natural grasslands exhibit frequent wildfires in some of the world's WUI, wildfires are not a concern where grasslands are highly managed pastures. In contrast, both managed and wild forests provide fuel for wildfires.

We found that the total global WUI area in 2020 was 6.3 million km² or 4.7% of global land area, which is an order of magnitude larger than the global urban area³⁷ or twice the size of India. The global land share of intermix and interface WUI is 3.6% (4.8 million km²) and 1.1% (1.5 million km²), respectively. Two thirds of the overall WUI area are dominated by forests, shrublands and wetlands, versus one third by grasslands. Globally, 3.5 billion people live within the WUI (1.7 billion in intermix

¹SILVIS Lab, Department of Forest and Wildlife Ecology, University of Wisconsin-Madison, Madison, WI, USA. ²Department of Biology and Environment, University of Haifa at Oranim, Kiryat Tivon, Israel. ³US Geological Survey, Geosciences and Environmental Change Science Center, Lakewood, CO, USA. ⁴Geography Department, Humboldt-Universität zu Berlin, Berlin, Germany. ⁵Integrative Research Institute on Transformations of Human-Environment Systems, Humboldt-Universität zu Berlin, Berlin, Germany. ⁶Institute of Geography and Spatial Management, Faculty of Geography and Geology, Jagiellonian University, Krakow, Poland. ⁷Northern Research Station, US Department of Agriculture Forest Service, Baltimore, MD, USA.  e-mail: fschug@wisc.edu

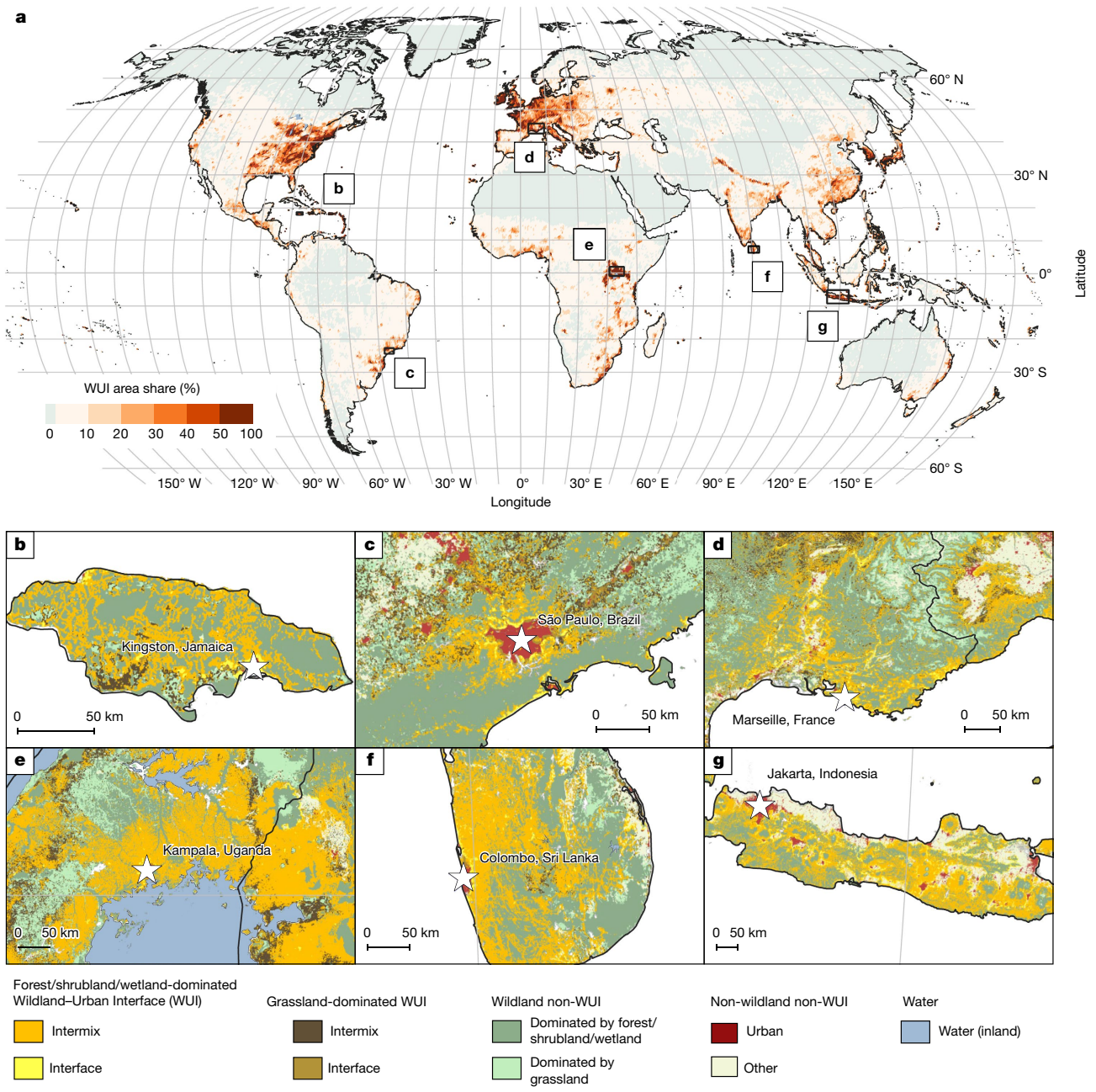


Fig. 1 | The global wildland–urban interface. **a**, Area share (%) of the WUI in about 2020 per hexagon with 50 km diagonal length. **b–g**, WUI and non-WUI map at 10 m resolution for parts of Jamaica (**b**), Brazil (**c**), France (**d**), Uganda (**e**),

Sri Lanka (**f**) and Indonesia (**g**). Interactive global map at <https://silvis.forest.wisc.edu/data/globalwui>. Land surface/country masks from <https://www.naturalearthdata.com>.

and 1.8 billion in interface WUI) and two thirds of those live in WUI dominated by forests, shrublands and wetlands. In total, nearly half of all buildings and people on the globe are potentially affected by the human–environmental hazards that are concentrated in the WUI. However, only 4.1% of the total aboveground living plant biomass occurs within the WUI, with most of it in the intermix WUI.

The WUI occurs on all continents. However, within continents, the distribution of the WUI is highly uneven. Large WUI areas occur along the Pacific coast of North America; in eastern North America and the Caribbean; along the Brazilian coast; across Europe; in West, South and East Africa, including Nigeria and Uganda; in Southeast Asia, including India, China, Indonesia and Japan; and in Australia (Fig. 1a). In some of these places, such as in California, Mediterranean Europe or South Africa, the WUI has been well studied because many buildings and people are affected by wildfires there^{38,39}. In many other places, however,

including East Africa, Brazil or Southeast Asia, widespread WUI has not been reported. Among the two most populated countries in the world, China has large WUI areas in southern and eastern regions, which are previously undocumented in the literature. However, India has much smaller WUI area in the southeast and the Himalayas, probably because cropland density is high in other regions⁴⁰, not providing enough wildland vegetation to create WUI. The area-adjusted overall accuracy of our WUI map is between 79.6% (when distinguishing all WUI classes) and 82.0% (when distinguishing WUI from non-WUI; Supplementary Data A).

The characteristics of the WUI vary considerably among continents. The WUI covers only 3% of South America but 15% of Europe. Europe and Asia have especially high shares of interface WUI area, whereas intermix WUI dominates in North America. South America is the only world region where grassland WUI area dominates, whereas Asia has the least.

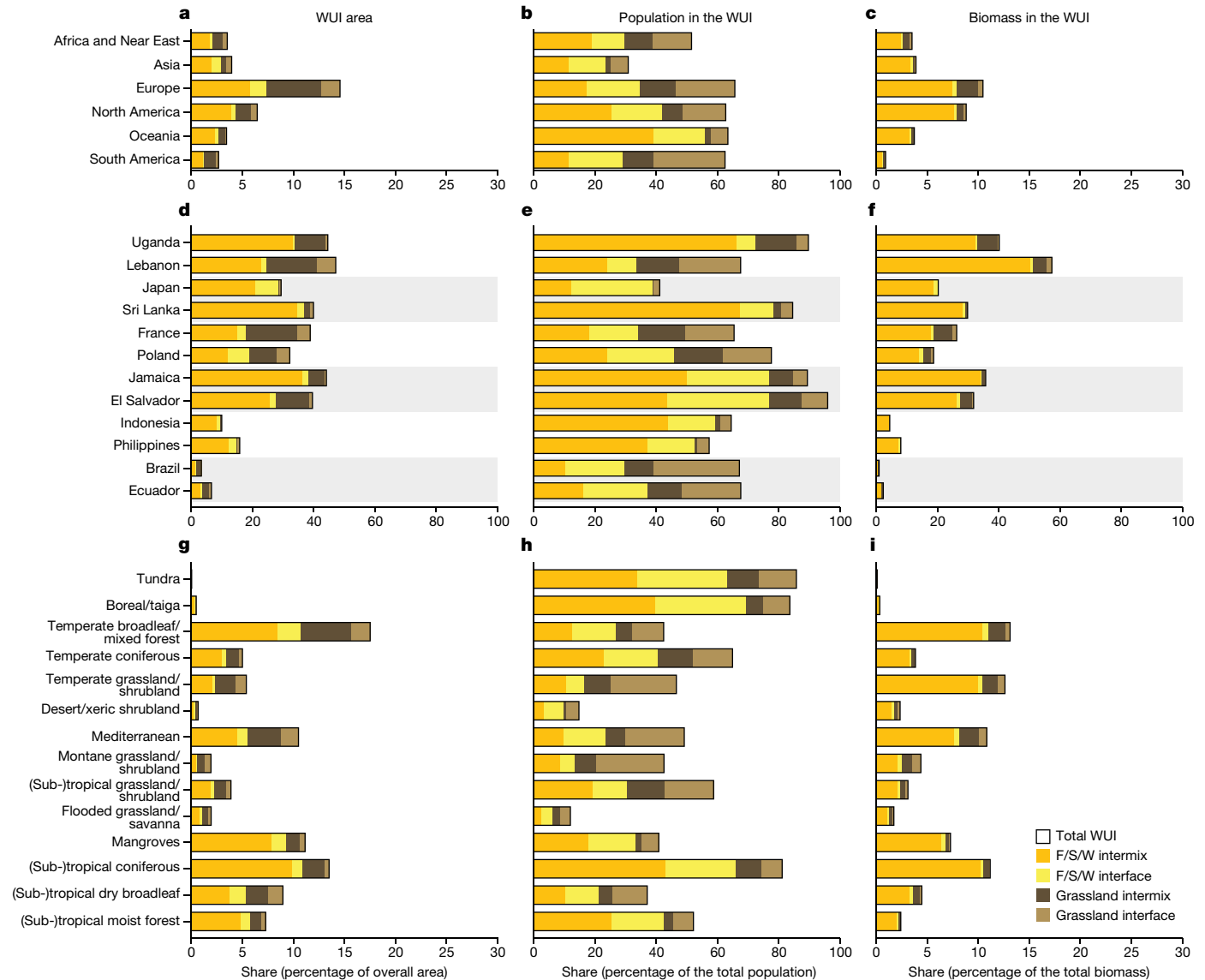


Fig. 2 | WUI area, population and biomass by world region, selected countries and biomes. **a–i**, Share of the WUI area in the total land area (**a, d, g**), share of population within the WUI (**b, e, h**) and share of biomass within the WUI per world region (**a–c**), selected country (**d–f**) and biome (**g–i**) (by latitude) as

defined by ref. 36. Shaded grey bars in **d, e** and **f** highlight world regions. F/S/W: dominated by forest/shrubland/wetland. Land surface/country masks from <https://www.natureearthdata.com>.

In South America, 33% of the population live in grassland-dominated WUI but only 7% in Asia. In Oceania, 56% of the total population lives in WUI dominated by forest, shrublands and wetlands, compared to only 24% in Asia. Europe has the largest share of its biomass, 10.5%, within the WUI (Fig. 2a–c). Seventy per cent of the global WUI area is in very low or low density rural areas and only 8% in urban clusters and centres (Extended Data Table 1, classes according to ref. 41). However, this pattern differs strongly by world region: in North America, 84% of the WUI is rural (5% in urban areas) but in Asia only 53% (14% in urban areas). Lastly, the WUI occurs in countries across all income classes (Extended Data Table 2).

We selected 12 hotspot countries on the basis of WUI area share and wildfire occurrence for closer examination: Uganda, Lebanon, Sri Lanka, Japan, France, Poland, Jamaica, El Salvador, Indonesia, the Philippines, Brazil and Ecuador (Fig. 1b–g, Extended Data Fig. 1 and Fig. 2d–f). Uganda, Sri Lanka, Jamaica and El Salvador have an exceptionally high share of population in the WUI (>80%) and many people there were affected by fires since 2003 (for example, 8.7 million in Uganda and 1.4 million in El Salvador). Lebanon has an exceptionally

high share of biomass in the WUI (60%) because most WUI occurs near its coastal regions where biomass is concentrated. In Japan, more than half of all wildfires occurred within the WUI and most of the people living in the WUI live in the interface because settlements are generally well demarcated and abut wildland vegetation. France and Poland have an especially high share of WUI area and population in the grassland WUI. In Indonesia, the Philippines, Brazil and Ecuador, WUI area share is small but high proportions of people live in those small WUI areas and are affected by wildfires (0.7 to 13.1 million, depending on the country). Those different WUI patterns reflect the diversity of reasons for both WUI development and wildfire occurrence and highlight that different management responses are required to mitigate the human–environmental conflicts that are concentrated in the WUI³.

Among biomes, the WUI is highly concentrated in a few (Fig. 2g–i and Extended Data Fig. 2). The temperate broadleaf and mixed forest biome covers only 9% of global land area, yet contains 35% of total WUI area. Similarly, subtropical and tropical moist broadleaf forests represent only 15% of the global land but contain 26% of WUI area. In contrast, deserts and xeric shrublands cover 20% of the land area but

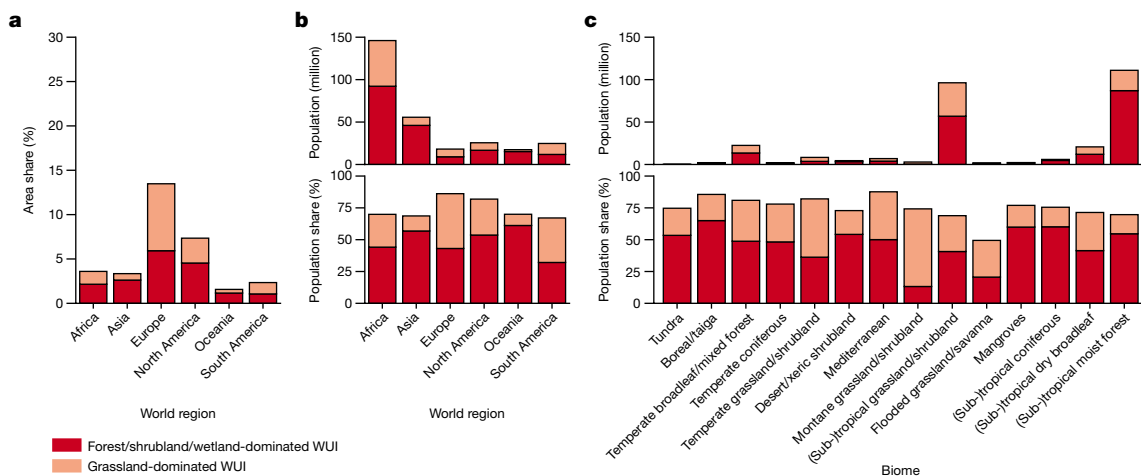


Fig. 3 | Wildfire in the WUI. **a**, Share of wildfire area within the WUI. **b**, Share of population (%) and number of all people that experienced wildfire within 1 km of their home that are within the WUI by world region. **c**, Share of population (%) and number of all people affected by wildfire that are within the WUI by biome (by latitude) as defined by ref. 36. Numbers according to MODIS active fire

contain only 3% of the global WUI area. We also observed large differences in population patterns: in both boreal forests/taiga and in subtropical and tropical coniferous forests over 80% of the population lives in the WUI, whereas in the deserts and xeric shrublands, only 10% does. The distribution of WUI area across biomes is important because WUI-related hazards, such as wildfires and their effects on people probably differ among biomes. Wildfire hazard is higher either where the WUI is widespread and where many people are affected by wildfire (such as in subtropical and tropical moist broadleaf forests) or where WUI area itself is small but both people and wildfires are concentrated there (such as boreal forests/taiga and mangroves that are highly vulnerable to fire). Wildfire hazard is also driven by the available biomass. In both the broadleaf/mixed forests and in subtropical and tropical coniferous forests, a substantial share of their biomass is in the WUI (about 13% in both biomes) as a result of their high overall share of land in the WUI (18% and 14%, respectively). By contrast, in the temperate grassland, savanna and shrubland biome, the overall WUI area share is low but a large portion of the biomass occurs in vegetation-rich coastal areas, which is also where the WUI is concentrated.

Wildfires are of increasing concern across the globe, as their frequency, intensity and season-length have increased because of climate change, more human ignitions and rising fuel loads⁴². Wildfires are particularly problematic in the WUI and cause substantial losses of houses and lives there⁴³. Indeed, more than two thirds of all people affected by wildfires during 2003–2020 (those experiencing a fire within 1 km of their homes) live in the WUI. This is partly because population density in the WUI is higher than in non-urban non-WUI areas but nevertheless substantial because only a small share of all global wildfire occurrences was directly in the WUI (Fig. 3a). Effects of WUI wildfires on the population differ among world regions and countries. In North America, 85% of the population affected by wildfire lives in the WUI but in Africa only 55% (nearly 150 million) does. In all world regions, except Europe and South America, most people were affected by wildfires that occurred in WUI dominated by forests, shrublands and wetlands (Fig. 3b). This suggests that, despite the WUI's small overall area, and, despite the comparatively rare occurrence of wildfires, buildings and people in the WUI may face an elevated wildfire hazard across the world.

The role of wildfires in the WUI differs among biomes but wildfire distribution suggests increasing effects of wildfires on people in the future. In some biomes, for example, in the tundra or in deserts and xeric shrublands, wildfires in the WUI are not a widespread phenomenon and

detection from 2003 to 2020. We analysed active fire point data in a 1 km grid and we considered all grid cells with at least one fire as being wildfire areas and all people living in a grid cell where a fire occurred 2003–2020 as affected by wildfire. Relative patterns are confirmed using VIIRS Active Fire data from 2013 to 2020 (Supplementary Data B–E).

relatively few people are affected (Fig. 3c). Some biomes, for example, Mediterranean forests, woodlands and shrublands, are small in area but are hotspots of recurring severe wildfire and destruction⁴². In other biomes, the large share of population living in the WUI (for example, 80% in boreal forests/taiga) and the fact that most people affected by wildfire during 2003–2020 lived in the WUI suggests that changing wildfire regimes could quickly increase the likelihood of wildfire exposure in the future. Particularly, there is a high probability that temperate broadleaf and mixed forests and subtropical and tropical moist broadleaf forests, the biomes with the largest WUI area and home to 130 million people previously affected by wildfire in the WUI, will experience increased fire hazard towards the middle of the twenty-first century if rising trends in wildfire fire frequency and intensity continue^{6,44–46}.

Discussion

The WUI is where people live within or near wildland vegetation. We found that the WUI covers nearly 5% of the global land area, even though the WUI has not been a class in any previous global land cover or land-use maps. We quantified the global extent of the WUI at high spatial resolution, characterized it by dominant land cover and related it to wildfires of the last two decades. Our analysis yielded three principal insights. First, we found that the WUI is a global phenomenon. Although previous work showed that the WUI is widespread in Mediterranean Europe, the United States and Australia², our results show large WUI areas in all continents, including previously undocumented hotspots in eastern Asia, East Africa and parts of South America. Second, the WUI is highly diverse in terms of population density, biomass quantity and dominant vegetation type. Third, the WUI is where wildfires affect the most people. Globally, two thirds of all the people that experienced wildfires live in the WUI. Among our WUI hotspots with frequent wildfires, many lack assessments of wildfire regimes, settlement patterns and wildfire risk, as is true for many WUI hotspots where wildfires are likely to become more prevalent as a result of changing climatic conditions.

Local and regional patterns of the WUI are highly variable. We found major differences in the proportion of area that is WUI in different countries, how many people live there, how much biomass occurs in the WUI and what the dominant land cover is. Although some WUI areas are well-known due to a history of disastrous wildfires (for example, Mediterranean areas of California and Europe and in Southeastern Australia),

we found many more places where the WUI is widespread. Some of these also have frequent wildfires, whereas other hazards and conflicts may dominate in other WUI areas. Furthermore, the patterns of the WUI vary greatly, from large continuous WUI areas in East Africa, stretching over hundreds of kilometres, to small and patchy WUI in the heterogeneous landscapes of Mediterranean Europe (Fig. 1d,e). Irrespective of whether a WUI area is large or small, it is likely to be a current or future hotspot of human–environmental conflicts affecting many people and many different types of ecosystems. As fire-prone areas expand globally, our WUI data can help guide proactive actions to prepare for future wildfire in the WUI and tailor such preparations according to the dominant vegetation types and associated fire regimes.

Wildfire damage to buildings is a global problem and we show that most people who experienced wildfire live in the WUI. This applies even in areas where wildfires are common but population density is low, such as in boreal forests or where wildfires are rare and few people live, such as in deserts. However, the subtropical and tropical moist forests, subtropical and tropical grasslands and shrublands and temperate broadleaf and mixed forests are the biomes where the most people live in the WUI and experienced wildfires. In these biomes, a future increase in the exposure of people to wildfire is probably due to (1) population and WUI growth⁴⁵; and (2) an increasing frequency of extreme weather events due to climate change, such as longer and more severe drought, causing lower fuel moisture and a higher frequency and severity of wildfires⁴⁶. How climate change affects wildfires will differ by vegetation type though. Grasslands, for example, can respond rapidly even to incremental climate change⁴⁷ and herbaceous fuels can increase rapidly after periods of high precipitation. Given that 15% of the global population lives in the grassland-dominated WUI, more intensive grassfires could become a big challenge for both wildfire preparedness and response⁴⁴.

Our WUI maps provide an accurate and high-resolution global perspective on a land-use type that is home to nearly half of the global population. The overall accuracy of our WUI maps was consistently high across regions and classes with only slight differences caused by uncertainties in the underlying building and land cover datasets (for example, 79% for Oceania versus 86% in Africa). Our WUI maps enable researchers to identify WUI hotspots where climate change, population growth, land-use change and increasing wildfire and other hazards are likely to cause the most pressing problems. Our maps are valuable because they offer a consistent global assessment at a resolution that is sufficiently fine to inform local and regional management, in addition to showing how global fire regimes are caused by and affecting humans⁴⁸. Future research will need to assess wildfire risk in the WUI in detail because that risk and the associated social vulnerability are affected by a multitude of factors, including land management practices, ecological and economic value, community preparedness, natural disturbance regimes, regional precipitation, temperature and vegetation patterns and wildfire management and prevention⁴⁹. For example, our maps treat both wild steppes and managed pastures as grasslands, yet the former are highly susceptible to wildfire whereas the latter are not. Similarly, our maps do not distinguish between natural forests and plantations, yet forest type can affect fire dynamics and wildfire likelihood. In WUI areas, fire risk can either increase as a result of higher fuel loads and more human ignitions or decrease as a result of fire suppression and fuel treatments, especially when buildings and people are threatened⁴⁵. The global WUI is, and will be, an area of both human–wildlife conflicts and coexistence. It is, thus, a key area to discover how to shape resilient, sustainable and livable settlements, in addition to minimizing human–environmental conflicts⁵⁰. Although fine-scale research is required to understand local drivers of WUI patterns, our globally consistent assessment highlights that WUI occurs on all continents, reveals its broad-scale patterns and provides a basis for future research on global WUI dynamics and the socioeconomic and biophysical processes that make the WUI unique.

Online content

Any methods, additional references, Nature Portfolio reporting summaries, source data, extended data, supplementary information, acknowledgements, peer review information; details of author contributions and competing interests; and statements of data and code availability are available at <https://doi.org/10.1038/s41586-023-06320-0>.

- Radeloff, V. C. et al. The wildland–urban interface in the United States. *Ecol. Appl.* **15**, 799–805 (2005).
- Bento-Gonçalves, A. & Vieira, A. Wildfires in the wildland–urban interface: key concepts and evaluation methodologies. *Sci. Total Environ.* **707**, 135592 (2020).
- Bar-Massada, A., Radeloff, V. C. & Stewart, S. I. Biotic and abiotic effects of human settlements in the wildland–urban interface. *BioScience* **64**, 429–437 (2014).
- Pesaresi, M. & Politis, P. *GHS Built-up Surface Grid, Derived From Sentinel2 and Landsat, Multitemporal (1975–2030)* (European Commission, Joint Research Center, 2022).
- Zanaga, D. et al. ESA WorldCover 10 m 2020 v100. *Zenodo* <https://zenodo.org/record/5571936> (2021).
- Ellis, T. M., Bowman, D. M. J. S., Jain, P., Flannigan, M. D. & Williamson, G. J. Global increase in wildfire risk due to climate-driven declines in fuel moisture. *Global Change Biol.* **28**, 1544–1559 (2021).
- Crutzen, P. J. Geology of mankind. *Nature* **415**, 23 (2002).
- Steffen, W., Crutzen, P. J. & McNeill, J. R. The Anthropocene: are humans now overwhelming the great forces of nature. *AMBIO* **36**, 614–621 (2007).
- Song, X.-P. et al. Global land change from 1982 to 2016. *Nature* **560**, 639–643 (2018).
- Winkler, K., Fuchs, R., Rounsevell, M. & Herold, M. Global land use changes are four times greater than previously estimated. *Nat. Commun.* **12**, 2501 (2021).
- Potapov, P. et al. Global maps of cropland extent and change show accelerated cropland expansion in the twenty-first century. *Nat. Food* **3**, 19–28 (2022).
- Melchiorri, M. et al. Unveiling 25 years of planetary urbanization with remote sensing: perspectives from the global human settlement layer. *Remote Sens.* **10**, 768 (2018).
- Elhacham, E., Ben-Uri, L., Grozovski, J., Bar-On, Y. M. & Milo, R. Global human-made mass exceeds all living biomass. *Nature* **588**, 442–444 (2020).
- Wiedenhofer, D. et al. Prospects for a saturation of humanity's resource use? An analysis of material stocks and flows in nine world regions from 1900 to 2035. *Global Environ. Change* <https://doi.org/10.1016/j.gloenvcha.2021.102410> (2021).
- Seto, K. et al. Urban land teleconnections and sustainability. *Proc. Natl Acad. Sci. USA* **109**, 7687–7692 (2012).
- Liu, J. et al. Framing sustainability in a telecoupled world. *Ecol. Soc.* <https://doi.org/10.5751/ES-05873-180226> (2013).
- Cohen, J. D. Preventing disaster—home ignitability in the wildland–urban interface. *J. For.* **98**, 15–21 (2000).
- Ganteaume, A., Barbero, R., Jappiot, M. & Maillé, E. Understanding future changes to fires in southern Europe and their impacts on the wildland–urban interface. *J. Saf. Sci. Resil.* **2**, 20–29 (2021).
- Radeloff, V. C. et al. Rapid growth of the US wildland–urban interface raises wildfire risk. *Proc. Natl Acad. Sci. USA* **115**, 3314–3319 (2018).
- Modugno, S., Balzter, H., Cole, B. & Borrelli, P. Mapping regional patterns of large forest fires in Wildland–Urban Interface areas in Europe. *J. Environ. Manag.* **172**, 112–126 (2016).
- Kaim, D., Radeloff, V. C., Szwagrzyk, M., Dobosz, M. & Ostafin, K. Long-term changes of the wildland–urban interface in the Polish Carpathians. *ISPRS Int. J. Geo-Inf.* **7**, 137 (2018).
- Li, S., Dao, V., Kumar, M., Nguyen, P. & Banerjee, T. Mapping the wildland–urban interface in California using remote sensing data. *Sci. Rep.* **12**, 5789 (2022).
- Argañaraz, J. P. et al. Assessing wildfire exposure in the Wildland–Urban Interface area of the mountains of central Argentina. *J. Environ. Manag.* **196**, 499–510 (2017).
- Sarricolea, P. et al. Recent wildfires in Central Chile: detecting links between burned areas and population exposure in the wildland urban interface. *Sci. Total Environ.* **706**, 135894 (2020).
- Vilà-Vilardell, L. et al. Climate change effects on wildfire hazards in the wildland–urban-interface—Blue pine forests of Bhutan. *For. Ecol. Manag.* **461**, 117927 (2020).
- Christ, S., Schwarz, N. & Sliuzas, R. Wildland urban interface of the City of Cape Town 1990–2019. *Geogr. Res.* **60**, 395–413 (2022).
- Bar-Massada, A., Radeloff, V. C., Stewart, S. I. & Hawbaker, T. J. Wildfire risk in the wildland–urban interface: a simulation study in northwestern Wisconsin. *For. Ecol. Manag.* **258**, 1990–1999 (2009).
- Kramer, H. A., Mockrin, M. H., Alexandre, P. M. & Radeloff, V. C. High wildfire damage in interface communities in California. *Int. J. Wildl. Fire* **28**, 641 (2019).
- Mietkiewicz, N. et al. In the line of fire: consequences of human-ignited wildfires to homes in the U.S. (1992–2015). *Fire* **3**, 50 (2020).
- Gavier-Pizarro, G. I., Radeloff, V. C., Stewart, S. I., Huebner, C. D. & Keuler, N. S. Housing is positively associated with invasive exotic plant species richness in New England, USA. *Ecol. Appl.* **20**, 1913–1925 (2010).
- Larsen, A. E., MacDonald, A. J. & Plantinga, A. J. Lyme disease risk influences human settlement in the wildland–urban interface: evidence from a longitudinal analysis of counties in the northeastern United States. *Am. J. Trop. Med. Hyg.* **91**, 747–755 (2014).
- Seto, K. C., Güneralp, B. & Hutyra, L. R. Global forecasts of urban expansion to 2030 and direct impacts on biodiversity and carbon pools. *Proc. Natl Acad. Sci. USA* **109**, 16083–16088 (2012).
- Jenerette, G. D. et al. An expanded framework for wildland–urban interfaces and their management. *Front. Ecol. Environ.* **20**, 516–523 (2022).
- Schoennagel, T. et al. Adapt to more wildfire in western North American forests as climate changes. *Proc. Natl Acad. Sci. USA* **114**, 4582–4590 (2017).

35. Liu, Z., Wimberly, M. C., Lamsal, A., Sohl, T. L. & Hawbaker, T. J. Climate change and wildfire risk in an expanding wildland–urban interface: a case study from the Colorado Front Range Corridor. *Landsc. Ecol.* **30**, 1943–1957 (2015).
36. Olson, D. M. et al. Terrestrial ecoregions of the world. A new map of life on Earth. *BioScience* **51**, 933 (2001).
37. Liu, X. et al. High-resolution multi-temporal mapping of global urban land using Landsat images based on the Google Earth Engine Platform. *Remote Sens. Environ.* **209**, 227–239 (2018).
38. Syphard, A. D., Clarke, K. C. & Franklin, J. Simulating fire frequency and urban growth in southern California coastal shrublands, USA. *Landsc. Ecol.* **22**, 431–445 (2007).
39. Chen, B. et al. Climate, fuel, and land use shaped the spatial pattern of wildfire in California's Sierra Nevada. *J. Geophys. Res.* <https://doi.org/10.1029/2020JG005786> (2021).
40. Hu, Q. et al. Global cropland intensification surpassed expansion between 2000 and 2010: a spatio-temporal analysis based on GlobeLand30. *Sci. Total Environ.* **746**, 141035 (2020).
41. Dijkstra, L. et al. Applying the degree of urbanisation to the globe: a new harmonised definition reveals a different picture of global urbanization. *J. Urban Econ.* **125**, 103312 (2021).
42. Pausas, J. G. & Keeley, J. E. Wildfires and global change. *Front. Ecol. Environ.* **19**, 387–395 (2021).
43. Calkin, D. E., Cohen, J. D., Finney, M. A. & Thompson, M. P. How risk management can prevent future wildfire disasters in the wildland-urban interface. *Proc. Natl Acad. Sci. USA* **111**, 746–751 (2014).
44. Knorr, W., Arneith, A. & Jiang, L. Demographic controls of future global fire risk. *Nat. Clim. Change* **6**, 781–785 (2016).
45. Bowman, D. M. J. S. et al. Vegetation fires in the Anthropocene. *Nat. Rev. Earth Environ.* **1**, 500–515 (2020).
46. Jolly, W. M. et al. Climate-induced variations in global wildfire danger from 1979 to 2013. *Nat. Commun.* **6**, 7537 (2015).
47. Barros, C., Thuiller, W. & Münkemüller, T. Drought effects on the stability of forest-grassland ecotones under gradual climate change. *PLoS ONE* **13**, e0206138 (2018).
48. Bowman, D. M. J. S. et al. The human dimension of fire regimes on Earth. *J. Biogeogr.* **38**, 2223–2236 (2011).
49. Chuvieco, E., Martínez, S., Román, M. V., Hantson, S. & Pettinari, M. L. Integration of ecological and socio-economic factors to assess global vulnerability to wildfire. *Global Ecol. Biogeogr.* **23**, 245–258 (2014).
50. Soulsbury, C. D. & White, P. C. L. Human–wildlife interactions in urban areas: a review of conflicts, benefits and opportunities. *Wildlife Res.* **42**, 541 (2015).

Publisher's note Springer Nature remains neutral with regard to jurisdictional claims in published maps and institutional affiliations.

Disclaimer Any use of trade, firm, or product names is for descriptive purposes only and does not imply endorsement by the U.S. Government.



Open Access This article is licensed under a Creative Commons Attribution 4.0 International License, which permits use, sharing, adaptation, distribution and reproduction in any medium or format, as long as you give appropriate credit to the original author(s) and the source, provide a link to the Creative Commons licence, and indicate if changes were made. The images or other third party material in this article are included in the article's Creative Commons licence, unless indicated otherwise in a credit line to the material. If material is not included in the article's Creative Commons licence and your intended use is not permitted by statutory regulation or exceeds the permitted use, you will need to obtain permission directly from the copyright holder. To view a copy of this licence, visit <http://creativecommons.org/licenses/by/4.0/>.

© The Author(s) 2023

Article

Methods

Defining the wildland–urban interface

Although the WUI is defined in different ways for different regions and applications^{19–24,51–54}, we used the conceptual WUI definition of the US Federal Register⁵³, first operationalized by ref. 1, which is the most widely used WUI definition in the United States and many other countries^{1,19–21,54}. This approach defines the intermix WUI as areas with more than 6.17 buildings per km² (or one building per 40 acres) and a wildland vegetation area share of greater than or equal to 50%. The interface WUI is defined as areas with more than 6.17 buildings per km² but less than 50% wildland vegetation that lie in proximity (less than 2.4 km) of a large patch (at least 5 km²) of wildland vegetation (with a share of more than 75%). The minimum patch size excludes small urban parks from wildland vegetation¹. The minimum distance of 2.4 km (1.5 miles) is included in the US Federal Register definition⁵³ and represents the distance embers can fly during a wildfire⁵⁵.

We further extended this WUI classification approach by stratifying WUI areas on the basis of the dominant land cover, into intermix or interface WUI dominated by forest, shrubland and wetland versus WUI dominated by grassland (Extended Data Fig. 3). We added that stratification because grasslands are among the most diverse and dynamic land cover types across the globe, with a large range of management practices, from wild steppe to managed pasture, almost resembling agricultural use^{56,57}. As a result, grasslands in a given place may or may not cause wildfire risk in the WUI, which is why previous national-level WUI maps purposefully either included⁵⁸ or excluded²¹ grasslands. Our separation of grassland-dominated WUI supports subsequent map interpretation.

Wildland vegetation and building data

We used two freely available global high-resolution datasets on land cover and buildings to map the WUI. Both datasets are derived from Earth observation satellite images and come in a raster format.

We used the European Space Agency WorldCover dataset to capture land cover information⁵. It is representative for 2020 (v.100) and provides land surface cover information distinguishing 11 classes globally with 10 m resolution. The overall accuracy of this dataset is about 75% (ref. 59). The information was derived from Sentinel-1 and Sentinel-2 satellite imagery using an ensemble of gradient-boosting decision trees with expert rule-based postprocessing to map many land cover classes at the same time (Supplementary Information)⁵.

We used the Global Human Settlement GHS-BUILT-S–R2022A dataset (hereafter, GHS-BUILT-S) as a reference for building location and density⁴. GHS-BUILT-S is representative for 2018 and provides pixel-wise estimates of built-up surface area (from 0% to 100% in steps of 1%) globally at 10 m resolution. The dataset contains all building types (with residential, commercial, industrial, agricultural, service or other purposes). The information was derived from Sentinel-2 satellite imagery using a symbolic machine learning approach designed to accurately capture built-up surface area (Supplementary Information).

We organized all spatial data in a data cube structure^{60,61} using the FORCE software⁶¹, matching the first tier of the EQUI7 reference grid⁶². This grid defines an equidistant projection for seven world regions (Africa, Antarctica, Asia, Europe, North America, Oceania and South America) divided into 100 km tiles. The grid facilitates mass data storage and efficient processing, meanwhile avoiding spatial grid oversampling and raster distortion. We used tiles over land for all EQUI7 world regions excluding Antarctica (Extended Data Fig. 4 and Supplementary Information).

Mapping the wildland–urban interface

We implemented a globally consistent workflow to map the WUI. Building on WUI-mapping approaches that use census block¹⁹ or building location data⁵⁴, we made some adaptations for our raster

data approach. Most notably, we could not apply the building density threshold of 6.17 km⁻².

We reclassified the land cover data into wildland versus non-wildland. Wildland vegetation included tree cover/forest, shrubland, grassland, herbaceous wetland, mangroves and moss and lichen. Non-wildland vegetation included cropland, built-up area, bare soil and sparse vegetation, snow and ice and water. For the interface WUI, we performed two reclassifications, where grassland was either included as wildland vegetation or not. Accordingly, we mapped two sets of large vegetation patches. We used the reclassified datasets to compute the wildland vegetation share within a circular kernel for intermix mapping (radius of 500 m following precedent)⁵⁴. We also identified patches of more than 5 km² where wildland vegetation share is greater than 75% for interface mapping. Pixels within 2,400 m (following precedent⁵⁴) of large vegetation patches were included as interface WUI.

On the basis of initial tests, we set building density to zero where slope is more than 25° (based on a gap-filled SRTM⁶³/ASTER⁶⁴ digital elevation model) or where intra-annual water occurrence in the Global Water Surface dataset⁶⁵ is more than 20%, that is, where water was present during at least 20% of the year to reduce commission errors on steep bare rock and in temporary river beds where false detections of buildings were more common (Supplementary Information). Also, we only considered pixels with an estimated building density of more than 20%, thereby removing areas with very low building density for which data accuracy can be limited. We defined all pixels with an aggregated building density greater than 0.5% in their surrounding (500 m radius) as candidate WUI pixels. Compared to the commonly used definition of 6.17 buildings per km², this threshold is usually slightly higher (depending on local building sizes). We chose this threshold to avoid WUI commission errors in low building density areas, which means that our WUI estimates are conservative. Similarly, we defined pixels with an average building density greater than 15% in a 500 m radius as having an urban character. These areas, for example, densely vegetated and high-density suburban environments, could not be classified as intermix WUI because urban vegetation often differs from wildland vegetation in terms of species identity, management practices and habitat restrictions and stronger fire control systems are in place that prevent fires. WUI mapping was subsequently performed as illustrated in Extended Data Fig. 3.

The WUI maps were masked where land cover was water. For intermix WUI, we determined the dominant land cover type within a pixel based on the area share of wildland vegetation. We distinguished pixels dominated by forests, shrubland and wetlands from those dominated by grassland.

We identified candidate hotspot countries as the top ten countries in their respective world region with the highest WUI area share, that had more than 20% of their wildfire area within the WUI and were more than 10,000 km² in size. Among these, we selected the two countries with the most people affected by wildfire in the WUI. If their borders were within 200 km, we replaced the second-ranked country with the third-ranked (until border distance greater than 200 km).

Population, biomass and fire

We analysed the extent and distribution of the global WUI and also calculated the population living in the WUI, proportion of biomass in the WUI and WUI area affected by wildfire.

For population data, we analysed the Global Human Settlement Population dataset (GHS-POP⁶⁶) that represents population per grid cell, with 100 m resolution. This dataset is based on the building density dataset we used to map the WUI but excludes non-residential buildings. It was created by disaggregating census data to grid cells using building density as weight. We computed area-weighted summaries of population data.

For biomass, we analysed global maps of aboveground biomass carbon density for 2010 (ref. 67), with 300 m resolution. We converted

biomass carbon density (MgC ha^{-1}) to mass (kg) and applied a factor of two to convert carbon equivalent mass to dry matter biomass⁶⁸. We computed area-weighted summaries of biomass data.

For wildfire data, we analysed the MODIS Collection 6.1 Active Fire dataset (MCD14ML)⁶⁹ and extracted grid cell-based fire frequency data from 2003 to 2020 (the years with complete data records for both Aqua and Terra). We selected only fires categorized as vegetation fires and excluded those representing active volcanoes and static land sources such as gas flares. Furthermore, we distinguished wildfires from agricultural or structural fires by only including fires for which the share of wildland vegetation in that MODIS pixel was more than 50% according to the WorldCover dataset. We reduced fire frequency data to fire presence by setting many fire occurrences within one grid cell to one. We defined a grid cell with fire presence as an area affected by wildfire. We used the MODIS Active Fire dataset because it provides the longest consistent spatially explicit global time series information of fire. However, MODIS active fire data have some limitations, for example caused by the wide sensor swath of 2,230 km, which can result in pixel area differences between nadir and the swath edges of a factor of 10, thereby potentially underestimating fire area at the swath edges⁷⁰. This is a particular issue as active fires are detected by thermal anomalies that, if classified as fire, are represented by a single point in the centre location of the pixel. Furthermore, its nominal pixel resolution of 1,000 m can result in the non-detection of small fires, particularly in low tree cover areas. This is why we also analysed data from the VIIRS Active Fire product which has 375 m spatial resolution since 2013. VIIRS data are comparable to the MODIS product but overcome some of its challenges as a result of higher resolution and narrower sensor swath⁷¹. We compared fire area and population affected by fire derived from VIIRS (2013 to 2020) or the MODIS data (2013–2020 for comparison and 2003–2020 for our main summary statistics).

Area correction

Where applicable, we used a pixel-based area-correction factor when computing area statistics to adjust skewed area statistics caused by our projection system (Supplementary Information).

Accuracy assessment and uncertainty

We evaluated the accuracy of the global WUI maps thoroughly using a stratified random sample⁷². Validation sites were stratified on the basis of the mapped area shares of our five classes: forest/shrub/wetland-dominated and grassland-dominated intermix and interface WUI and non-WUI. We conducted our validation independently for each of the six world regions based on expert-opinion reference data derived from the visual interpretation of submetre to metre resolution satellite imagery available in Google Earth.

According to ref. 72, the number of required validation sites is based on the mapped area proportion W_i of each validated class i , the target user's accuracy U_i and the target standard error S for the estimated overall accuracy (equation (1)).

$$n = \left(\frac{\sum_{i=0}^5 (W_i \times \sqrt{U_i \times (1 - U_i)})}{S} \right)^2 \quad (1)$$

The number of sites n was drawn for each world region. The sites were then equally allocated to the five classes. A class-area proportion of the distribution would have complicated data handling, as non-WUI was expected to be by far the dominant class. The total number of validation sites was 1,504 per world region, that is, 300 or 301 per world region and class, based on a target user's accuracy of 0.75 and a target standard error of 0.01. The sites were randomly drawn within the respective strata (Extended Data Fig. 5).

The overall area-adjusted mapping accuracy when distinguishing WUI versus non-WUI classes was 82.1% (Extended Data Fig. 6). The

area-adjusted overall accuracy when all five classes were separately assessed was 79.6%. Class-wise user's and producer's accuracies ranged considerably and so did overall accuracies without area-adjustment (Supplementary Data A). Area-adjusted accuracy is largely affected by the high area share and high user's accuracy of the non-WUI class, whereas all WUI classes have a minor area share across the globe. The overall accuracy varied only slightly among the world regions (between five and ten percentage points), with no clear recurring patterns. The overall accuracy between different interpreters differed by similar margins. Only 3% of all validation points were labelled as 'uncertain' during the validation process. The quality of the WUI map is largely a function of the quality of the underlying land cover data. For example, despite the overall high accuracy of the ESA WorldCover product, the user's accuracy of shrublands, one of the key land cover types for WUI mapping, is only 39% (ref. 59). The quality of our WUI map also depends on the quality of building data. However, we found that because WUI requires only to be above the minimum building density threshold, even fairly widespread omission errors in areas with scattered buildings typically do not lead to missed WUI. On the other hand, in areas where small, isolated buildings are missed, the mapped WUI area was not greatly affected either because such isolated buildings do not form WUI even when mapped correctly.

We also compared our global WUI map with previously generated census-based and building location-based WUI maps across the United States^{19,54} and found high agreement in total WUI area (Pearson correlation of 0.80) (Extended Data Fig. 7a). In densely populated northeastern states (for example, Connecticut, Massachusetts, New Jersey and Rhode Island), we found considerably more WUI area than census-based and building location-based approaches. In most other states, our WUI area estimate is very close to or slightly higher than estimates from the census-based approach and slightly lower than from the building location-based approach. We also compared our map results with data from two previous studies across 36 European countries^{20,73} and found high agreement in total WUI area with ref. 27 ($r = 0.94$ across all countries) and medium agreement with ref. 20 ($r = 0.55$) (Extended Data Fig. 7b). However, in Europe, we consistently map more WUI than those two studies. Compared to ref. 73, we mapped more WUI because our distance threshold for interface mapping is larger (2.4 km versus 0.6 km) and ref. 20 defined the WUI as the overlap of the buffers around built-up land cover (200 m buffer) and vegetation (400 m buffer), which resulted in considerably less WUI.

We developed our WUI maps on the basis of a well-established definition of the WUI that was originally developed in the United States and successfully applied in other world regions (for example, Argentina^{23,74} and Poland²¹) However, WUI maps depend on the mapping criteria, especially the radius that is considered when computing mean building density for a given area and the distance to a large vegetation patch that determines the interface WUI. Previous sensitivity analyses confirmed the general suitability of the parameters that we selected, that is, a 500 m radius for density calculations and a 2,400 m distance to a large vegetation patch. In the United States, radii smaller than 500 m make the resulting WUI maps highly sensitive to commission or omission errors in the underlying building dataset, whereas larger radii resulted in minimal changes in WUI area⁵⁴. In Europe, overall WUI area is 25% lower when limiting interface WUI to areas within 600 m of a large vegetation patch compared to 2,400 m but WUI area estimates based on either distance were highly correlated ($R^2 = 0.94$; ref. 73). Because there are no published WUI-mapping thresholds for most parts of the globe, we decided to apply the most established approach across the globe but acknowledge the value of further regionalized research that accounts for local particularities.

The comparison of wildfire area in the WUI and population affected by wildfire between the MODIS Active Fire and the VIIRS Active Fire datasets showed very similar patterns for both. Globally, 3.1% of wildfire area is in the WUI according to MODIS (2013–2020), compared to

Article

3.5% in VIIRS (2013–2020), with a difference of less than 2.6 percentage points in any world region. The slight difference is probably due to the ability of VIIRS to capture smaller fires and potentially more fires in areas located at the MODIS swath edges (see Supplementary Data B–E for more detailed information and comparisons by biome, region, country and subnational administrative units).

Data availability

All raster data are available in a public data repository (<https://zenodo.org/record/7941460>). The data are also accessible at <https://geoserver.silvis.forest.wisc.edu/geodata/globalwui>. We share the data for visualization purposes in an interactive data view at <https://silvis.forest.wisc.edu/data/globalwui>. Source data are provided with this paper.

Code availability

The algorithm to map the WUI with our raster-based approach is shared here and in the data publication: https://github.com/franzschug/global_wildland_urban_interface.

51. Lampin-Maillet, C. et al. Mapping wildland–urban interfaces at large scales integrating housing density and vegetation aggregation for fire prevention in the South of France. *J. Environ. Manag.* **91**, 732–741 (2010).
52. Zambrano-Ballesteros, A., Nanu, S. F., Navarro-Carrión, J. T. & Ramón-Morte, A. Methodological proposal for automated detection of the wildland–urban interface: application to the Metropolitan regions of Madrid and Barcelona. *ISPRS Int. J. Geo-Inf.* **10**, 381 (2021).
53. Forest Service, Bureau of Indian Affairs, Bureau of Land Management, Fish and Wildlife Service & National Park Service. *Urban Wildland Interface Communities Within the Vicinity of Federal Lands That Are at High Risk From Wildfire* (Forest Service, USDA, 2001).
54. Carlson, A. R., Helmers, D. P., Hawbaker, T. J., Mockrin, M. H. & Radeloff, V. C. The wildland–urban interface in the United States based on 125 million building locations. *Ecol. Appl.* **32**, e2597 (2022).
55. Platt, R. V. The wildland–urban interface: evaluating the definition effect. *J. For.* **108**, 9–15 (2010).
56. Bengtsson, J. et al. Grasslands—more important for ecosystem services than you might think. *Ecosphere* **10**, e02582 (2019).
57. Bardgett, R. D. et al. Combatting global grassland degradation. *Nat. Rev. Earth Environ.* **2**, 720–735 (2021).
58. Mockrin, M. H., Helmers, D., Martinuzzi, S., Hawbaker, T. J. & Radeloff, V. C. Growth of the wildland–urban interface within and around U.S. National Forests and Grasslands, 1990–2010. *Landsc. Urban Plan.* **218**, 104283 (2022).
59. Tsendbazar, N. et al. *WorldCover Product Validation Report* (WorldCover, 2021); https://worldcover2020.esa.int/data/docs/WorldCover_PVR_V1.1.pdf.
60. Lewis, A. et al. Rapid, high-resolution detection of environmental change over continental scales from satellite data—the Earth Observation Data Cube. *Int. J. Digital Earth* **9**, 106–111 (2016).
61. Frantz, D. FORCE—Landsat + Sentinel-2 analysis ready data and beyond. *Remote Sens.* **11**, 1124 (2019).
62. Bauer-Marschallinger, B., Sabel, D. & Wagner, W. Optimisation of global grids for high-resolution remote sensing data. *Comput. Geosci.* **72**, 84–93 (2014).
63. Earth Resources Observation and Science Center. *USGS EROS Archive—Digital Elevation—Shuttle Radar Topography Mission (SRTM) 1 Arc-Second Global* (Earth Resources Observation and Science Center, 2017).
64. Abrams, M., Crippen, R. & Fujisada, H. ASTER Global Digital Elevation Model (GDEM) and ASTER Global Water Body Dataset (ASTWBD). *Remote Sens.* **12**, 1156 (2020).
65. Pekel, J.-F., Cottam, A., Gorelick, N. & Belward, A. S. High-resolution mapping of global surface water and its long-term changes. *Nature* **540**, 418–422 (2016).
66. Schiavina, M., Freire, S. & MacManus, K. *GHS-POP R2022A – GHS Population Grid Multitemporal (1975–2030)—OBSOLETE RELEASE* (European Commission, Joint Research Centre, 2022).
67. Spawn, S. A. & Gibbs, H. K. *Global Aboveground and Belowground Biomass Carbon Density Maps for the Year 2010* (ORN DAAC, 2020); <https://doi.org/10.3334/ORNDAAC/1763>.
68. Petersson, H. et al. Individual tree biomass equations or biomass expansion factors for assessment of carbon stock changes in living biomass—a comparative study. *For. Ecol. Manag.* **270**, 78–84 (2012).
69. Giglio, L., Schroeder, W. & Justice, C. O. The collection 6 MODIS active fire detection algorithm and fire products. *Remote Sens. Environ.* **178**, 31–41 (2016).
70. Schroeder, W. et al. Characterizing vegetation fire dynamics in Brazil through multisatellite data: common trends and practical issues. *Earth Interact.* **9**, 1–26 (2005).
71. Schroeder, W., Oliva, P., Giglio, L. & Csaszar, I. A. The New VIIRS 375 m active fire detection data product: algorithm description and initial assessment. *Remote Sens. Environ.* **143**, 85–96 (2014).
72. Olofsson, P. et al. Good practices for estimating area and assessing accuracy of land change. *Remote Sens. Environ.* **148**, 42–57 (2014).
73. Bar-Massada, A., Alcasena, F., Schug, F. & Radeloff, V. C. The wildland–urban interface in Europe: spatial patterns and associations with socioeconomic and demographic variables. *Landsc. Urban Plan.* **235**, 104759 (2023).
74. Godoy, M. M. et al. Rapid WUI growth in a natural amenity-rich region in central-western Patagonia, Argentina. *Int. J. Wildl. Fire* **28**, 473 (2019).

Acknowledgements We thank D. Frantz for computing the gap-filled SRTM/ASTER digital elevation model, for advice on area-correction factors when computing area statistics in the EQUI7 projection and on biomass data processing. This study was funded by the NASA Land Cover and Land Use Change Program under agreement 80NSSC21K0310. D.K. acknowledges the support of the National Science Centre, Poland, contract no. UMO-2019/35/D/HS4/00117.

Author contributions Conceptualization was by F.S. and V.C.R. Methodology was developed by F.S., D.H., A.C. and H.C. Investigation was undertaken by F.S. and K.P. Validation was done by N.K., H.C., K.P., S.M., F.S. and D.H. Visualization was by F.S., D.H., K.P. and H.C. Funding acquisition was by V.C.R. Resources were obtained by V.C.R. and D.H. Project administration was by V.C.R. and F.S. The original draft was written by F.S., with review and editing carried out by F.S., V.C.R., D.H., A.C., H.C., K.P., N.K., S.M., A.B.-M., T.H., P.H., D.K. and M.M.

Competing interests The authors declare no competing interests.

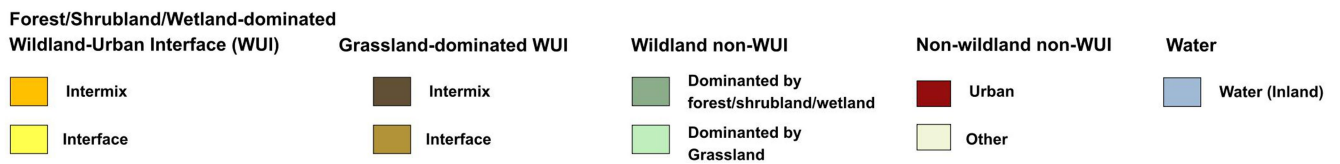
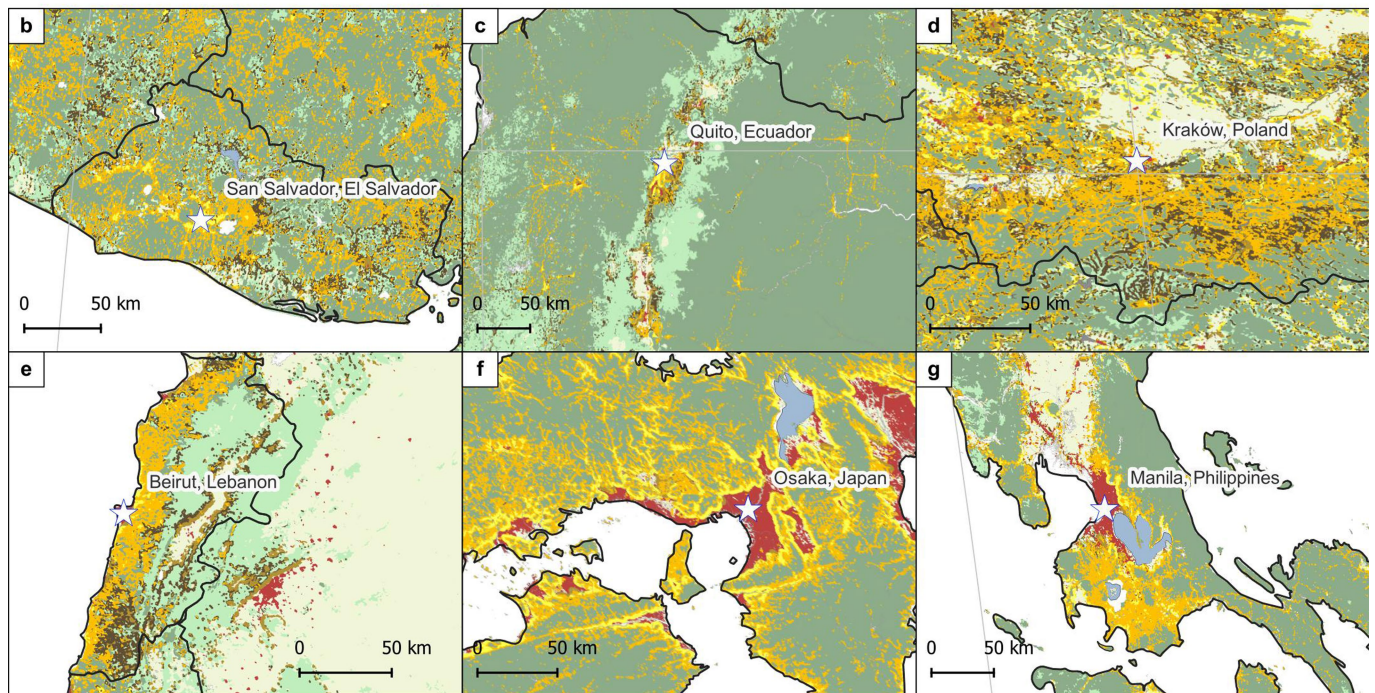
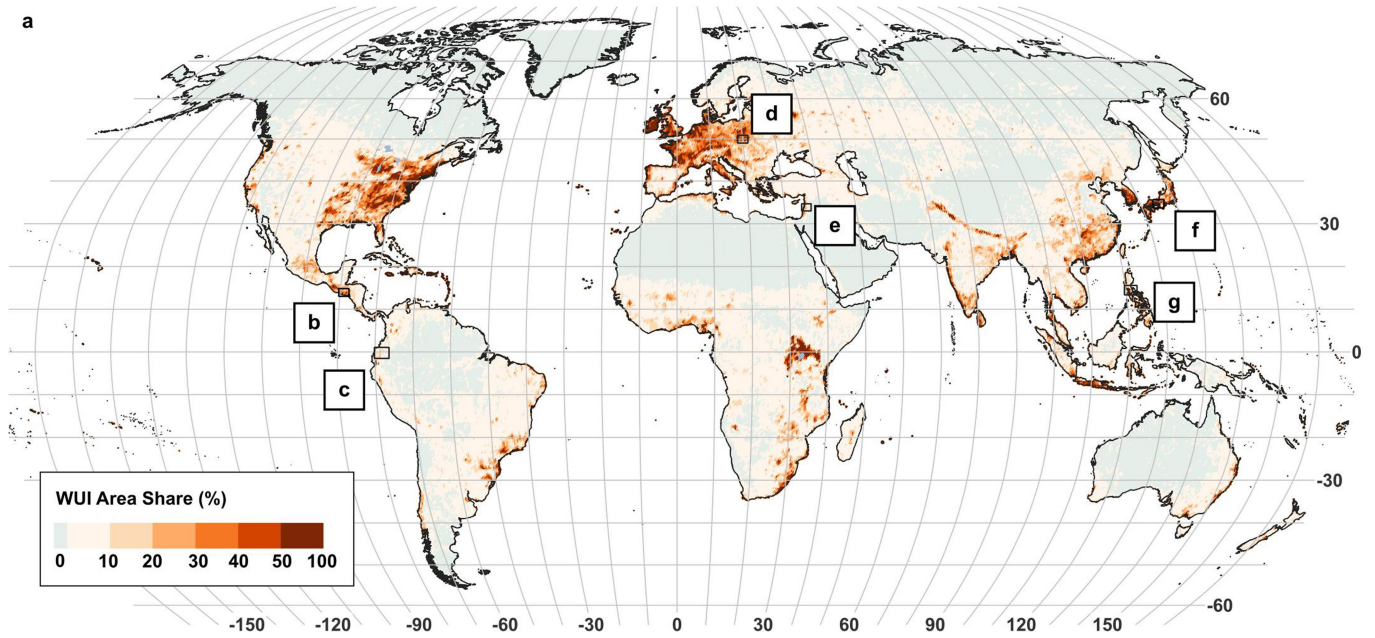
Additional information

Supplementary information The online version contains supplementary material available at <https://doi.org/10.1038/s41586-023-06320-0>.

Correspondence and requests for materials should be addressed to Franz Schug.

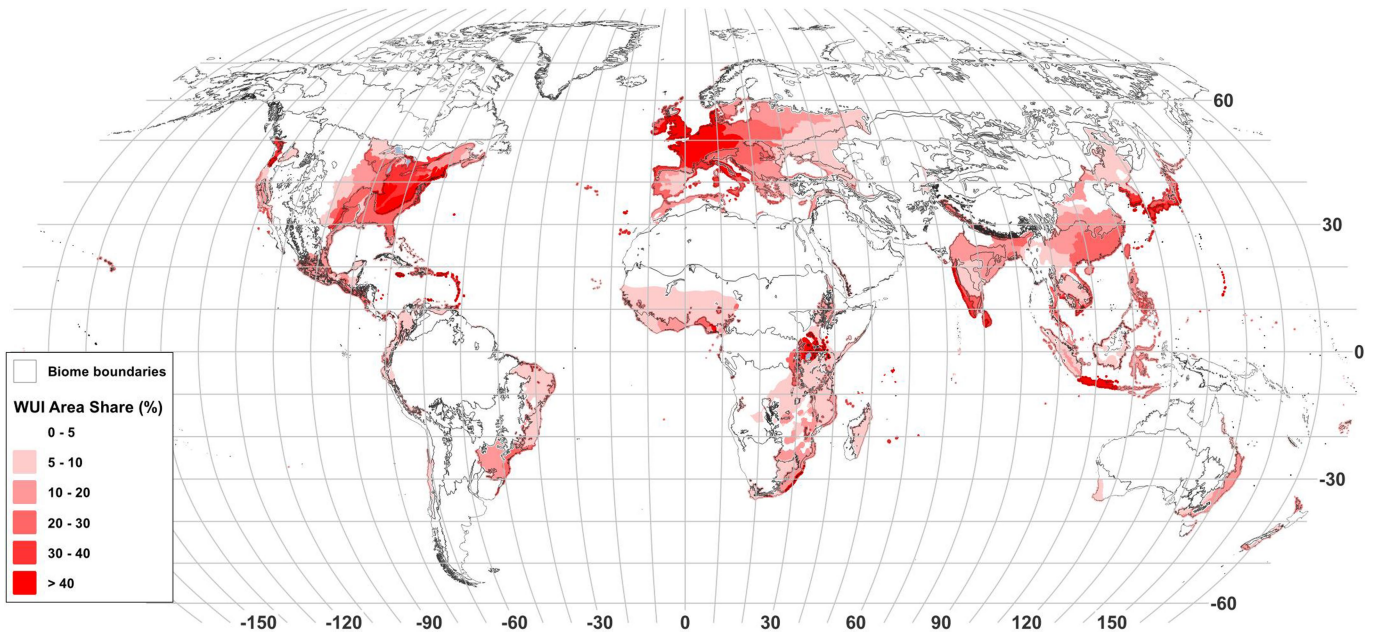
Peer review information *Nature* thanks Kirsten Thonicke and the other, anonymous, reviewer(s) for their contribution to the peer review of this work.

Reprints and permissions information is available at <http://www.nature.com/reprints>.

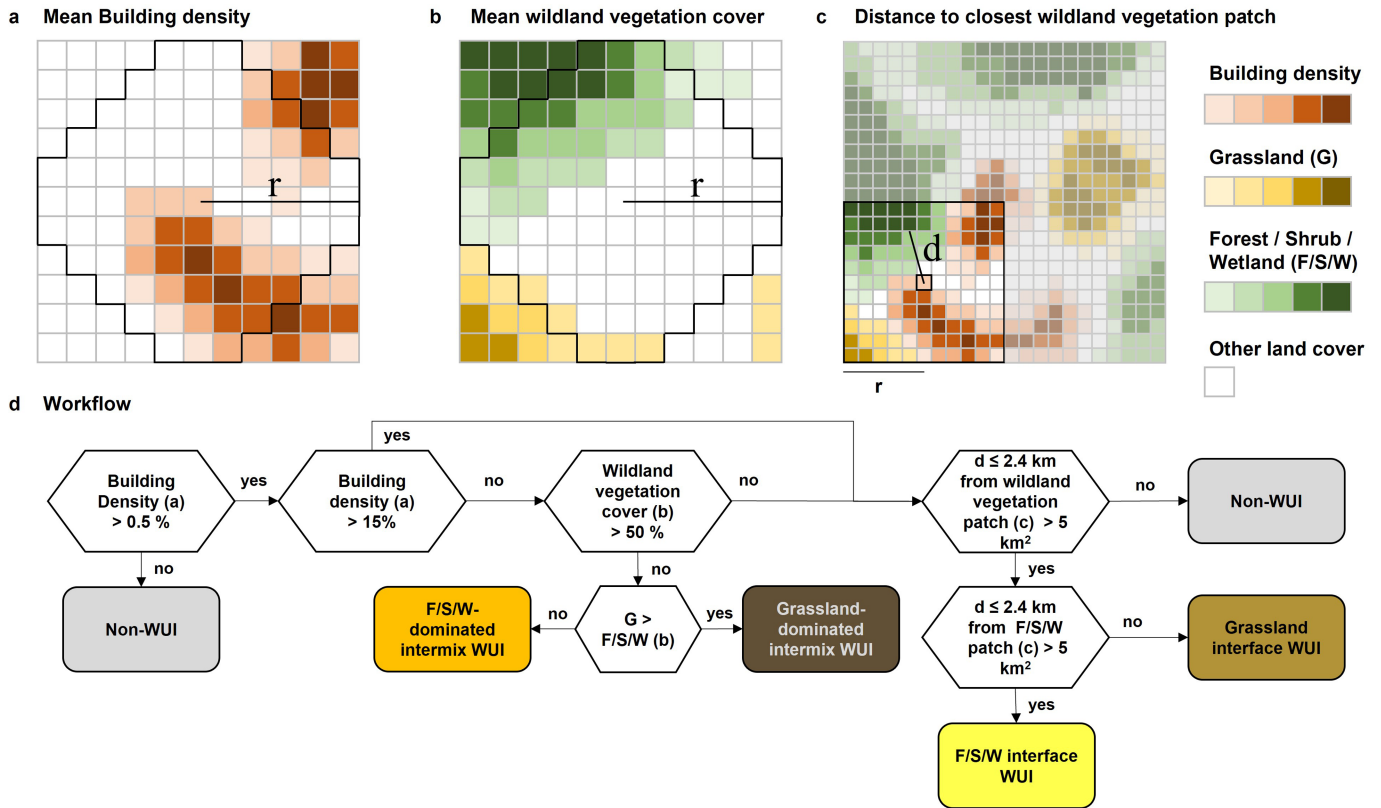


Extended Data Fig. 1 | The global Wildland–Urban Interface. **a**, Area share (%) of the Wildland–Urban Interface (WUI) in ca. 2020 per hexagon with 50 km diagonal length. **b–g**, WUI and non-WUI map at 10 m resolution for parts of

El Salvador (**b**), Ecuador (**c**), Poland (**d**), Lebanon (**e**), Japan (**f**), and the Philippines (**g**). Interactive global map at <https://silvis.forest.wisc.edu/data/globalwui/>.

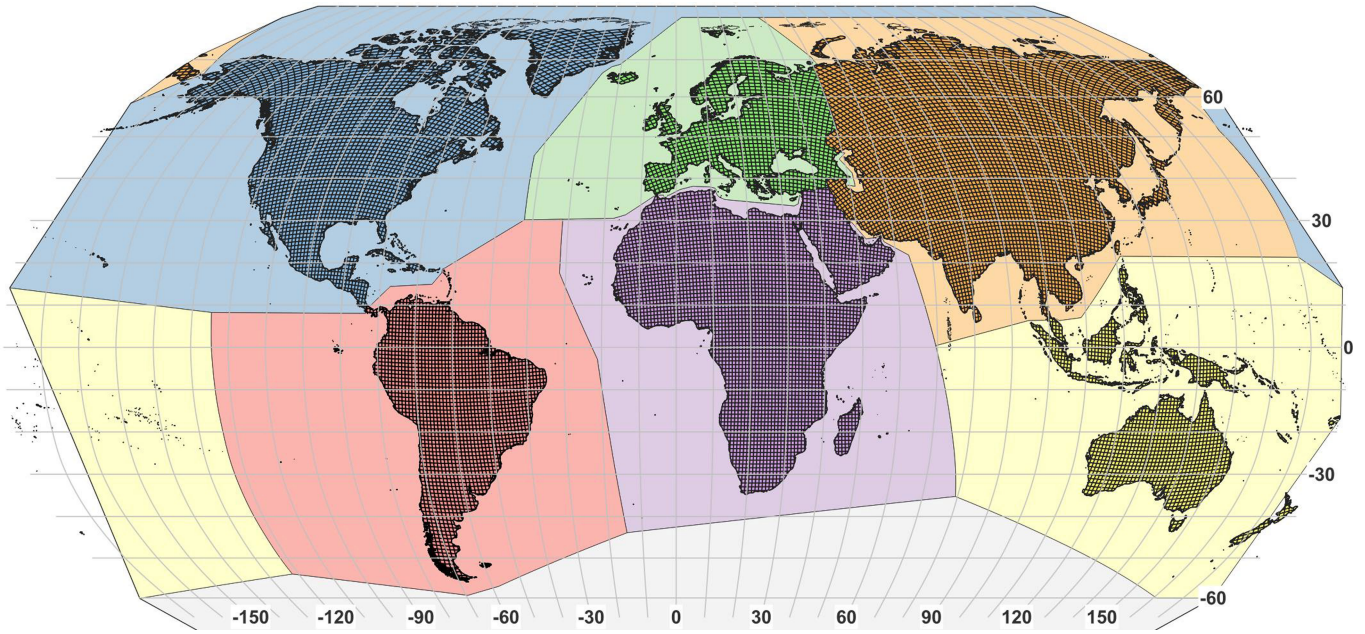


Extended Data Fig. 2 | WUI area share by biome. Per cent area share of the total of the four mapped WUI classes per biome. Black lines: Biome boundaries as defined by Olson et al. (2001)³⁶. Map projection: Robinson. Grid coordinates: WGS 84.



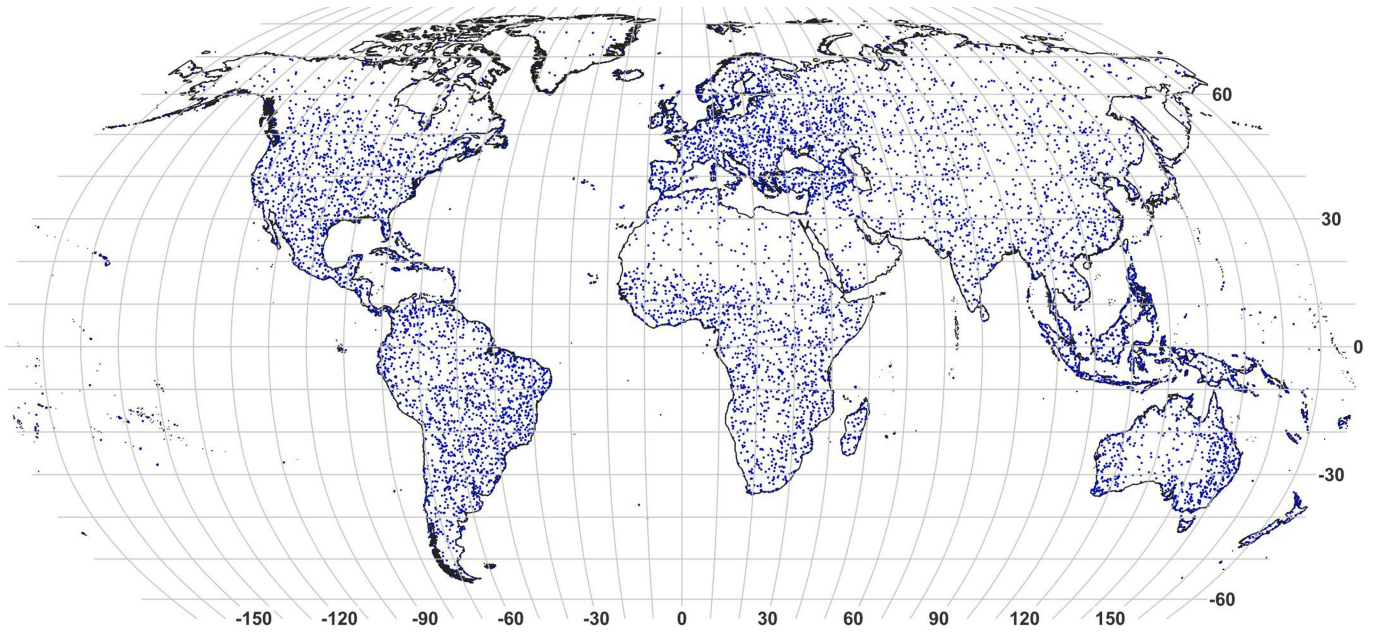
Extended Data Fig. 3 | The Wildland-Urban Interface mapping workflow. Classifying the Wildland-Urban Interface based on **a**, moving window mean building density and **b**, wildland vegetation in a circular kernel (r = radius = 500 m, black outline) and **c**, distance to the closest large wildland vegetation

patch (d = distance = 2,400 m). G = grassland, $F/S/W$ = forest/shrubland/wetland. **d**, Combining building density and wildland vegetation to map the Wildland-Urban Interface.

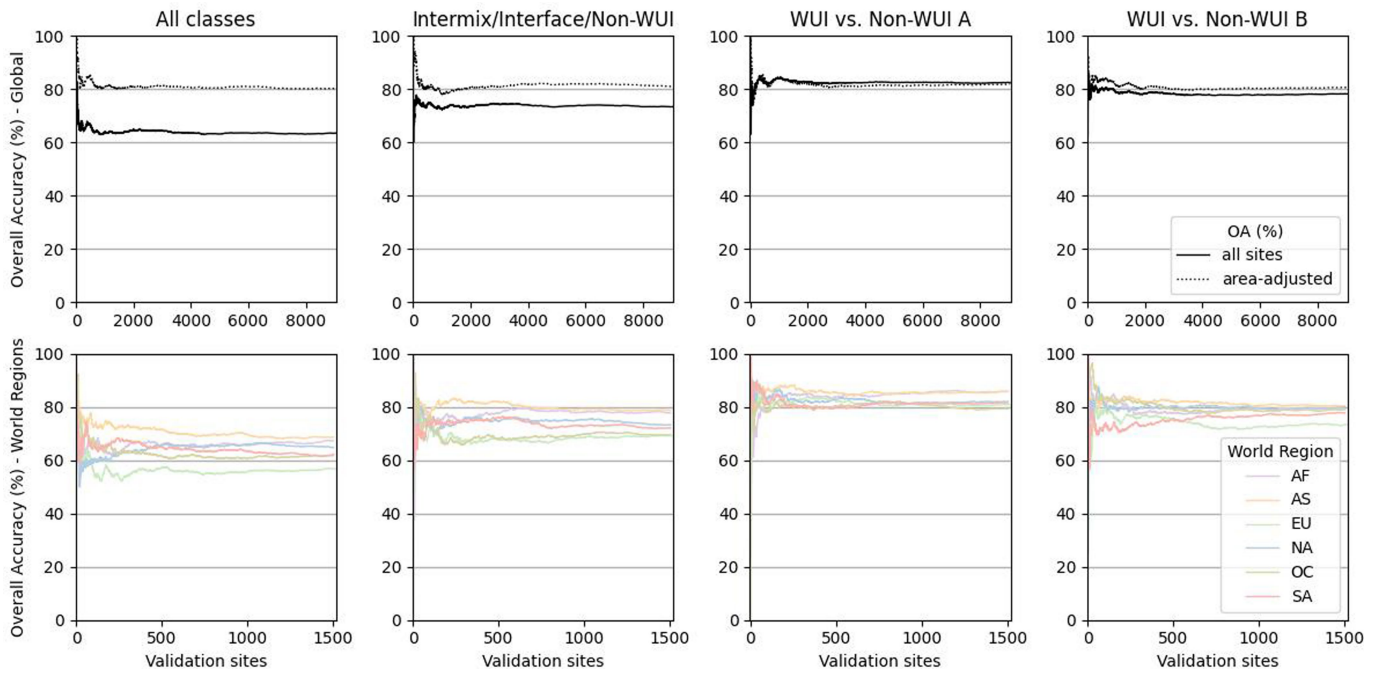


Extended Data Fig. 4 | World regions and tiling scheme, EQUI7 reference grid. Tile counts: Africa – 3814 (purple), Asia – 4547 (orange), Europe – 1374 (green), North America – 3155 (blue), Oceania – 2026 (yellow), South America –

2055 (red). Adapted from Bauer-Marschallinger et al. (2014)⁶². Map projection: Robinson. Grid coordinates: WGS 84.

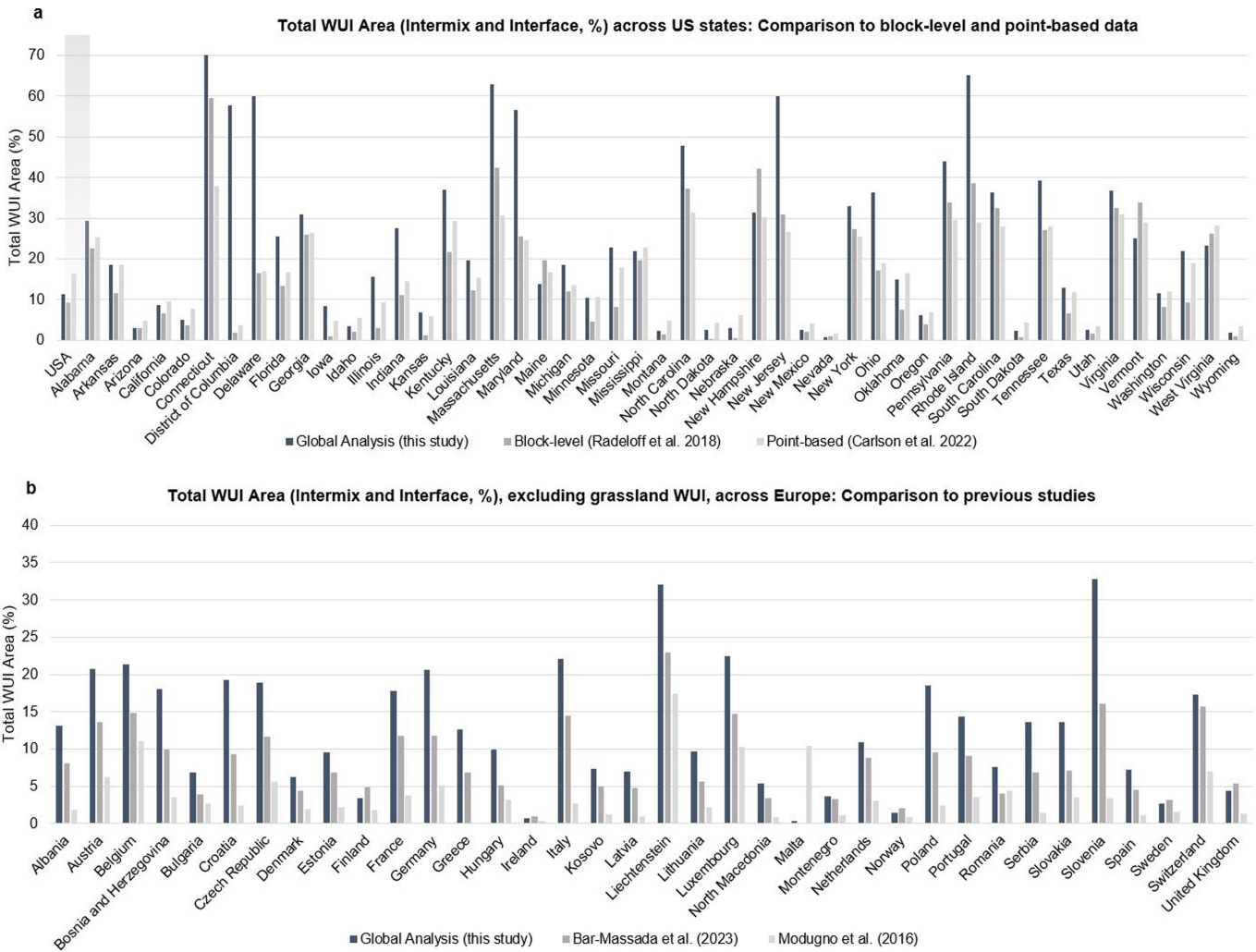


Extended Data Fig. 5 | Global Wildland–Urban Interface, Validation Sites. Global distribution of all validation sites, 1,504 per world region for a total of 9,024, world regions defined according to Extended Data Fig. 4. Map projection: Robinson. Grid coordinates: WGS 84.



Extended Data Fig. 6 | Overall Accuracy of global Wildland-Urban Interface (WUI) mapping. Iterative overall and area-adjusted accuracy (%) globally (top) and by world region (bottom). Columns represent different class aggregations. All classes (left): all mapped classes individually (non-WUI, forest/shrubland/wetland-dominated intermix WUI, grassland-dominated intermix WUI, forest/

shrubland/wetland-dominated interface WUI, grassland-dominated interface WUI). Intermix/Interface/Non-WUI (centre left): intermix and interface classes aggregated respectively. WUI vs. Non-WUI A (centre right): all WUI classes aggregated. WUI vs. Non-WUI B (right): aggregates forest/shrubland/wetland-dominated WUI as WUI, and grassland-dominated WUI as non-WUI.



Extended Data Fig. 7 | Total WUI area comparison with previous studies states in the conterminous United States and for selected European countries.

a, Comparison of aggregated global mapping results for 48 conterminous US states to Census block-level and building centroid point-based WUI mapping (Radeloff et al. 2018⁴⁹, Carlson et al. 2022⁵⁷). The data in Radeloff et al. are representative for 2010. The data in Carlson et al. are representative for 2015–2018. **b**, Comparison for 36 European countries: The data in Modugno et al.

are representative for 2006²⁰. The data in Bar-Massada et al. are representative for 2019–2020⁷². Neither European study considers grassland areas as wildland vegetation. Differences in WUI area share are due to smaller distance thresholds for WUI Interface mapping (600 m distance to closest large vegetation patch in Bar-Massada et al.⁷³) and lower mapping resolution with a simplified buffering approach for building detection (only buffer overlaps of built-up land cover and vegetation are considered WUI in Modugno et al.²⁰).

Article

Extended Data Table 1 | The global Wildland–Urban Interface and the degree of urbanization

World Region	WUI Area (%) in very low / low density rural areas	WUI Area (%) in rural clusters	WUI Area (%) in suburban or peri-urban	WUI Area (%) in dense and semi-dense urban cluster	WUI Area (%) in urban center
Africa and Near East	66.1	8.8	15.1	6.5	3.5
Asia	53.0	7.4	25.7	8.4	5.5
Europe	79.1	5.2	7.9	4.5	3.2
North America	84.1	2.9	7.5	3.8	1.7
Oceania	56.3	6.0	23.4	7.5	6.6
South America	78.4	4.6	7.1	4.6	5.3

WUI area in different degree of urbanization classes. Classes according to Dijkstra et al. (2021⁴¹).

Extended Data Table 2 | The global Wildland–Urban Interface and income

World Bank Income Group	WUI Area Share (%)	Population in the WUI (%)	Biomass in the WUI (%)	Population affected by fire in the WUI (%)
High Income	6.5	58.1	9.6	87.5
Upper Middle Income	3.4	45.4	1.9	75.2
Lower Middle Income	5.5	36.0	4.9	70.4
Low Income	3.4	56.2	2.8	65.5

WUI Area Share, Share of population and biomass in the WUI as well as population affected by fire in the WUI per World Bank Income Group 2023 (<https://datahelpdesk.worldbank.org/knowledgebase/articles/906519-world-bank-country-and-lending-groups>).